Hydro-Mechanical Loading and Compressibility of Fibrous Media for Resin Infusion Processes

P. Ouagne, Joel Breard, Tariq Ouahbi, Abdelghani Saouab, C.H. Park

Hydro-Mechanical Loading and Compressibility of Fibrous Media for Resin Infusion Processes

P. Ouagne[1,2,*], J. Bréard[1], T. Ouahbi[1], A. Saouab[1], C.H. Park[1]

[1]*Laboratoire Ondes et Milieux Complexes, FRE 3102 CNRS, Université du Havre,*
53 rue de Prony, 76058 Le Havre France
[2]*Present address: Institut PRISME, Polytech'Orleans*
8 rue Leonard de Vinci, 45072 Orleans France
[*]*Corresponding author: pierre.ouagne@univ-orleans.fr; Tel + 33 2 38 41 73 32; Fax: +33 2 38 41 73 29*

Abstract

The modelling of composite manufacturing processes where hydro-mechanical coupling takes place depends on the validity of compressibility and permeability models. In this work, the computer code initially used to simulate the effect of coupled hydro-mechanical load on composite preform [2] is integrated into an inverse method to predict the compaction behaviour of the reinforcements. An experimental device developed at Le Havre is used to apply hydro-mechanical loads to the preforms. Two ramps of stress are imposed to the preform and the thickness evolution is measured as a function of time. The speed of thickness reduction is not constant and varies in the range of 0.1 to 12 mm/min. The effect of compression speed upon the saturated fabrics is investigated. For a fixed fibre volume fraction, an increase in stress is observed in increasing compression speed. The experimental results are compared to the compressibility curves determined by an inverse method. The calculated curves correspond to the compressibility curves experimentally obtained with low compression speed (~ 0.25 mm/min). As a consequence, this suggests that a low compression speed should be applied when investigating the compressibility behaviour of composite preform with a view of modelling resin infusion processes.

Keywords: Composite reinforcements, Compressibility, Inverse method, Hydro-Mechanical loading

1 Introduction

1.1 LCM Processes/ Resin Film Infusion

The need for manufacturing large composite parts in the aeronautic industry is ever increasing. For this reason, Liquid Composite Molding (LCM) processes are widely used. These processes consist of injecting a liquid thermoset resin through some layers of a dry and shaped preform. Within the LCM processes, two main classes can be distinguished. In the first one, RTM and variants (CRTM, RTMlight …) can be found, whereas infusion and variants (VARI, LRI, RFI …) is the basis of the second class.

Figure 1 shows the process conditions of several LCM processes. The mould can be rigid or semi rigid. The consolidation of the composite part can be controlled under stress or displacement condition. The direction of resin flow can be longitudinal (L), longitudinal-transverse (L+T) or transverse (T). A positive or negative pressure can also be applied to favor the impregnation of resin.

A process such as the RFI (Resin Film Infusion) is well adapted to large part manufacturing. The infusion processes such as RFI [3] consists of transmitting a stress through a vacuum bag to a stack of semi-cured liquid resin film and dry preform (Figure 2). The whole set up is generally placed in an autoclave to ensure the correct compaction stress and to control the temperature cycle. The resin flows through the preform in the direction of the applied stress.

1.2 Process Modelling

The process is controlled by stress conditions. The reinforcement compressibility and the resin flow occur simultaneously and there is thus a mutual influence between the

two phases of solid and liquid. A strong hydro-mechanical coupling between the reinforcement compaction and the resin flow takes place and should be taken into account in the process modelling. Hydro-mechanical coupling also takes place during the CRTM process, for example. In this process, a constant speed is applied on the upper mould. The process is controlled by displacement conditions.

There have been several studies dealing with the modelling of resin infiltration in deformable preforms under different conditions [4-6]. In these works, the fabric was supposed to be uniformly deformed in the direction of applied stress. In processes such as RFI, the principal resin flow and fabric deformation occur in the same direction. The resin pressure and the fabric compaction stress are not uniform along the thickness direction. The differentials of pressure and compaction stress in the z direction are taken into account in the modelling of the RFI process proposed by Ouahbi *et al.* [2]. A Model using similar basis was also proposed by Park and Kang [7]. Independently of simulating the RFI process, the computer code proposed by Ouahbi *et al.* [2] was developed to predict the evolution of the reinforcement's thickness submitted to various combination of hydraulic and mechanical loading (Hydro-Mechanical loading) as a function of time.

1.3 Hydro-Mechanical coupling Modelling

Table 1 shows the set of equations required to model processes where transverse hydro-mechanical coupling takes place. The basis of all models is the mass conservation equation (eq. 1), where q is the relative resin velocity, V_f the fibre volume fraction and u_s the solid velocity. This mass conservation equation is derived from mass conservation equations of resin and fibre (Appendix A). The resin flow through the

fibrous reinforcement is a typical example of flow through a porous media, which, on the macroscopic scale, is well described by Darcy's law (eq. 2) [8]. The fluid velocity q and the pressure gradient ∇p are linearly related by the resin viscosity μ and the transverse permeability of fibrous medium K_Z. Equation (3) describes the stress balance between the effective stress σ'_Z received by the fibrous skeleton, the pressure applied to the resin pressure p and the stress applied to the whole system σ_Z. F_c and F_p are the function to relate respectively compressibility C_Z and permeability K_Z of fibrous medium versus fibre volume fraction (eq. 4 and eq. 5).

1.4 Fabric compaction behaviour

Table 1 indicates that it is necessary to estimate fabric behaviours parameters such as the compressibility C_Z and the permeability K_Z to model processes where hydro-mechanical coupling takes place. The previously mentioned models [2, 4-6] are based on experimentally determined material properties. The compressibility as well as the permeability behaviour of the preform is key entry parameter to the process modelling.

Numerous experimental studies dealt with the compressibility of dry or lubricated fibrous reinforcements (Robitaille and Gauvin [9], Kelly *et al.* [10]). These authors have shown that the stress induced by the compression of fibrous reinforcements depends on the compression speed applied and the level of lubrication of the preforms. Indeed, fibrous preforms can be considered as visco-elastic materials and the stress induced by the compression under displacement conditions of the preform is dependent on the strain rate applied to the system.

The compressibility behaviour of the preform is generally modelled by empirical laws. The Toll and Manson model [11] based on a power law formulation is frequently used and is given by Equation 5 with $F_c = cV_f^d$ where c and d are the coefficients of the power law.

Merhi et al. [12] proposed a "physical" explanation based on the beam theory for the value of d in the case of randomly aligned fibre bundles mat. For other types of reinforcements, the d value is obtained from experimental curves of compressibility. Luo *et al.* [13] and Toll et al. [11] found b values situated in the range 5-8 for mats, and in the range 9-15 for more ordered reinforcements such as UD (unidirectional) or woven fabrics. Moreover, the value of c can be greatly affected by the variation of compression speed due to the viscoelastic response of the reinforcements in compression [14].

As stated previously, a mathematical model for the compressibility behaviour of the reinforcement has to be defined a priori, for the purpose of modelling. In fact, the experimental measurement of compression behaviours shows a dependency on the strain rates applied during the test and on the degree of impregnation of the preform. Furthermore, the compressibility behaviour of a dry preform is different than the one of saturated-by-a-fluid preform. Indeed, lubrication mechanisms favour the rearrangement of tows and fibre during compression.

In processes such as C-RTM (Compression Resin Transfer Moulding), the compression of the preforms takes place under displacement conditions. The mould compression speed can generally be controlled and fixed. As a consequence, it is possible to evaluate experimentally the compressibility and to use the compressibility model in the

numerical simulation. In processes such as RFI, where the compression is applied under stress conditions, the speed of compression is not constant. It is, therefore, difficult to correctly validate a fabric compressibility model that should be used in the process simulation tool.

2 Scope of the study

2.1 Compressibility model in the RFI process

In this work, it is proposed to investigate numerically the compressibility curve corresponding to a hydro-mechanical consolidation applied under stress conditions (as in the RFI process) and to compare it with a set of experimental compressibility curves determined under displacement conditions with different compression speeds. To this objective, the computer code developed by Ouahbi *et al.* [2] is incorporated into an inverse method. The parameters *c* and *d* of the Toll and Manson model are determined by an iterative method. The model parameters are updated in an iterative way by minimizing the difference between measured thickness values and the computed thickness values with current model parameters following Equation 6.

$$S(c,d) = \frac{1}{2}\sum_{i=1}^{N}\left[\frac{H_i^c(c,d) - H_i^m}{H_i^m}\right]^2 \tag{6}$$

where H_i^c and H_i^m are the computational and the measured thickness at the *i*th time step. *N* is the number of measurements and *c*, *d* are the coefficients of the power law.

The *c* and *d* coefficients are repeatedly updated through the optimization procedure.

The optimization problem is solved by the Levenberg-Marquardt method [15]. To evaluate the sensitivity coefficients, the gradient is approximated by central difference scheme.

The response to hydro-mechanical loading is the main input parameter for an inverse method to investigate the compressibility behaviour of reinforcements. The transverse permeability of the fibrous reinforcements is the second input parameter. The experimental evaluation of the transverse permeability was performed by several authors such as Drapier *et al.* [16], Scholz *et al.* [17]. Ouagne *et al.* [18] presented transverse permeability models for reinforcements of different natures and architectures and the results on the material studied in this work are used.

2.2 Hydro-mechanical loading/process conditions

The experimental device was designed to apply transverse hydro-mechanical loads to fibrous reinforcements. Different combinations of fluid flow rates and mechanical stresses can be imposed to the fibrous preforms. The fibrous reinforcements are submitted to a hydraulic load. In this study, a constant flow rate is applied. The reinforcements are also submitted to mechanical loads. These loads can be applied either under stress conditions (a fixed or a ramp of stress is applied and the displacement of the fibrous reinforcement measured), or under displacement conditions (a displacement rate is applied and the stress induced is measured).

The behaviour of reinforcements submitted to hydro-mechanical loads are presented and discussed. The results are then used as input parameter in the model developed by Ouahbi *et al.* [2] to investigate the compressibility behaviour of the studied material.

The result given by the model can be compared to experimental compressibility curves determined by applying a constant velocity load on saturated reinforcements.

3 Experimental procedures

3.1 Experimental device

A device was set up at Le Havre to simultaneously establish hydraulic and mechanical loads (Hydro-Mechanical coupling loads) to the fibrous preforms (Figure 3). This apparatus consists of a stainless steel cylindrical pot within which a guided piston induces the exact amount of fibres compaction in the transverse direction. The device is mounted on a universal testing machine (Instron 8802) to control the displacement speed of the piston or the stress applied to the fibrous medium. The fluid is guided in the transverse direction by perforated bronze grids. The device is designed to apply to the reinforcements either a flow rate or a pressure. A pressure transducer is placed below the lower grid. Test samples of fibrous preforms are placed between the two grids. A pressure pot can be used to apply a constant pressure to the reinforcements. A six litre syringe is placed on a universal testing machine (Instron 5867) in order to apply a controlled flow rate of silicon oil to the fibrous reinforcement. The magnitude of the flow rate is controlled by the Instron 5867 crosshead speed. When a newtonian test fluid such as silicon oil is injected at a constant flow rate through the fibrous reinforcement, a pressure rise at the reinforcement entry is measured by the pressure sensor.

3.2 Race tracking

A study was carried out to determine if race tracking was taking place along the walls of the cylinder. To this objective, different flow rates were imposed to fibrous preforms of constant fibre volume fraction and the corresponding rises of pressure were recorded. A

silicon joint was used to avoid race tracking along the walls of the cylinder. The efficiency of this joint was confirmed by the linearity of the flow rate versus pressure (Figure 4). Indeed, if race tracking was taking place along the cylinder walls, the rise of pressure would not be proportional anymore to the imposed flow rate. In this case the pressure rise would be "slower" than the rise of flow rate. Deviation from linearity in the flow rate-pressure relationship has been checked for all the fibre volume fractions but only one graph is shown in Figure 4.

3.3 Calibration

A preliminary study was carried out for different flow rates to quantify the pressure rise due to the fluid flow going through the bronze grid. The rise of pressure for each flow rate was then deducted when hydro-mechanical loads are imposed to fibrous preforms.

3.4 Material and experimental conditions

The material used during this study was an E glass 5 harness satin weave. This material has an areal weight of 620 g/m^2 and an initial fibre volume fraction of ~ 48%. The thickness of an individual layer of fabric is 0.5 mm. The fluid used in the experimental procedure was silicon oil with a viscosity of 0.1 Pa.s. A specially made cutter was machined to obtain circular preforms of an accurate size. The different layers of fabric were superimposed and the yarns of each layer are placed parallel to the corresponding yarns of the neighbouring fabric layer. Twenty layers of fabric were disposed for each test. The compaction velocity was ranged from 0. 5 to 2 mm/min for the saturated compression tests (reinforcements in a bath of silicon oil) and a velocity of 0.5 mm/min was used for hydro-mechanical coupling tests under displacement condition. Under

stress condition, hydro-mechanical tests were conducted following ramps of 5 kN/min and 10 kN/min up to a load of ~ 30 kN where the load was held constant to observe eventual visco-elastic recovery. For hydro-mechanical coupling tests, a constant flow rate (6.7 10^{-6} m^3/s) was obtained by keeping the syringe speed constant.

The transverse permeability behaviour of the studied material is presented in Figure 5 and is extracted from the results presented in [18].

4 Results and Discussion

4.1 Hydro-mechanical coupling under stress condition

Under stress condition, the variation of thickness due to a constant mechanical stress rate is measured as a function of time. A fluid flow of constant flow rate is also applied to place the specimen of fabric under hydro-mechanical load. Figure 6 shows the variation of thickness of same specimen submitted to two different load rates (corresponding to 0.63 and 1.3 MPa/min stress rates) up to a load of 3.8 MPa. When the ramp of mechanical stress is applied, the two curves show a fast decrease of the reinforcement thickness over about 10 seconds with apparent constant speeds. During the first 10 seconds, the upper grid travels a distance of about 2 mm therefore conferring an average speed of 12 mm/min. Between t = 310 s and t = 480 s for the 10 kN/min curve and between t = 310 s and t = 660 s for the 5 kN/min curve, the piston progressively slows down while being still submitted to the same stress rate and same constant flow rate. However, the thickness of preforms does not reach a constant value. The final compression speed measured for the curve submitted to the 5 kN/min rate is about 0.1 mm/min before the load reaches a value of 3 MPa. The final compaction

speed measured for the curve submitted to the 10 kN/min rate is about 0.15 mm/min. This demonstrates that during the compression at constant stress rate, the speed of compaction changes from about 12 to 0.1 mm/min. This suggests that for a given fibre volume fraction, the value of the effective stress received by the fibrous skeleton may be different. The modelling of the hydro-mechanical coupling under stress condition may require the knowledge of a wide range of compression curves determined under different displacement speeds.

In terms of micromechanisms, the acceleration of the lower grid (between t ~ 300 and t ~310 s) with increasing applied stress is probably due to a quick fibre rearrangement and filling up of the porosity. Then, the rearrangement of the fibres becomes probably more and more difficult due to a higher level of fibre compression and lower porosity.

Figure 6 also shows that the final thickness of the samples submitted to the faster stress ramp is lower than the sample submitted to a slower stress ramp. This confirms that the 5 harness satin glass weave exhibits a strong visco-elasticity.

4.2 Hydro-mechanical coupling under displacement conditions

4.2.1 Experimental hydro-mechanical coupling

Figure 7 shows the experimental response of the fibrous reinforcements submitted to saturated compression and to hydro-mechanical coupling under displacement condition. In both cases, hydro-mechanical coupling takes place as a flow of fluid is induced by compressing the porous medium. The speed of compression is the same for both tests (0.5 mm/min), and the flow rate of silicon oil is kept constant throughout the hydro-mechanical coupling test. Figure 7 shows that the saturated compression and hydro-

mechanical coupling curves exhibit similar trends. The difference in the experimental conditions results from the application of a flow rate for the hydro-mechanical coupling test. The flow of silicon oil exits from the device by a pipe of sufficient diameter. The values of stress recorded by the machine load cell would be higher if the exhaust pipe has a lower diameter.

4.2.2 Identification of compressibility by inverse method

An inverse method is applied to determine the model parameters for the experimental hydro-mechanical curves obtained under stress conditions. The computed results of *c* and *d* parameters in Toll and Manson model are shown in Table 2.

The influence of compression speed on saturated compression tests is shown on Figure 8. The stresses required to compress the same fibrous preforms increases with an increasing compaction speed as already mentioned by Robitaille and Gauvin [9] for dry compression of satin glass weave. This demonstrates the visco-elastic behaviour of fibrous *E* glass satin weave preforms submitted to hydro-mechanical loads.

Ouahbi *et al.*'s [2] simulation tool is integrated into an inverse method to establish the compressibility curves corresponding to the two hydro-mechanical curves shown in Figure 6. Those simulated compressibility curves are used as input parameter for the hydro-mechanical model used this time in its original form. The evolution of the reinforcement thickness submitted to two different stress ramps is compared to hydro-mechanical coupling experimental results. A good agreement is observed between the computed thickness evaluated from the compressibility parameters previously estimated using the inverse method (Table 2) and the measured thickness determined experimentally by applying hydro-mechanical loads under stress conditions (Figure 9).

In Figure 8, the compressibility curves obtained from the inverse method are compared to experimental curves determined with imposed compression velocities (between 0.25 to 2 mm/min). The compressibility curves, determined numerically by using the inverse method, shows similar shapes than experimental compressibility curve determined with an imposed compression speed of 0.25 mm/min.

This implies that the compressibility behaviour required to model hydro-mechanical coupling should be experimentally determined under a slow imposed compression speed.

If the parameter d in Toll and Manson model is considered to be fixed for a given preform and to be dependent of the reinforcement microstructure, then the coefficient c should vary to accommodate the visco-elasctic effects such as the ones observed with compression speed changes. It is therefore proposed to replace the constant c by a visco-elastic function to establish a behaviour model to take into account the effects induced by changes in the loading conditions.

5 Conclusions

A computer code initially used to simulate the effect of coupled hydro-mechanical load on composite preform is incorporated into an inverse method to estimate the compressibility behaviour of the reinforcements. An experimental device developed at Le Havre is used to apply hydro-mechanical loads to the preforms. Two ramps of stress are imposed to the preform and the thickness evolution is measured as a function of time. The speed of thickness reduction is not constant and varies in the range 12 to 0.1

mm/min. The effect of compression speed upon saturated reinforcements is investigated. For a fixed fibre volume fraction, an increase in stress is observed when increasing compression speeds. The experimental results are compared to the compressibility curves determined by inverse method. The calculated curves show a behaviour corresponding to compressibility curves experimentally obtained with low compression speed (~ 0.25 mm/min). As a consequence this suggests that a low compression speed should be applied when investigating the compressibility behaviour of composite preform with a view of modelling infusion processes.

References

1. Bréard J, Saouab A. Numerical simulation of liquid composite molding Processes, *European Journal of Computational Mechanics* 14 (2005) 841-865.
2. Ouahbi T, Saouab A, Bréard J, Ouagne P, Chatel S. Modeling of hydro-mechanical coupling in infusion processes. *Composites Part A* 38 (2007) 1646-1654.
3. Antonucci V, Giordano M, Nicolais L, Calabro A, Cusano A, Cutolo A, Inserra S. Resin flow monitoring in Resin Film Infusion process. *Journal of Materials Processing Technology* 143-144 (2003) 687-692.
4. Correia NC, Robitaille F, Long AC, Rudd CD, Simacek P, Advani SG. Analysis of the vacuum infusion moulding process: I. Analytical formulation. *Composites Part A* 36 (2005) 1645–56.
5. Lopatnikov S, Simacek P, Gillespie J, Advani SG. A closed form solution to describe infusion of resin under vacuum in deformable fibrous porous media. *Modelling and Simulation in Materials Science and Engineering* 12 (2004) 191–204.

6. Sommer JL, Mortensen A. Forced unidirectional infiltration of deformable porous media. *Journal of Fluid Mechanics* 22 (1996) 1205–22.

7. Park J. and Kang MK. A numerical simulation of the resin film infusion process. *Composite Structures* 60 (2003) 431-437.

8. Darcy H. Les fontaines publiques de la ville de Dijon. *Dalmont*, Paris, 1856.

9. Robitaille F, Gauvin R. Compaction of textile reinforcements for composites manufacturing. I: Review of experimental results. *Polymer Composites* 19 (1998) 198-216.

10. Bickerton S, Buntain MJ, Somashekar AA. The viscoelastic compression behaviour of liquid composite molding performs. *Composites Part A* 34 (2003) 431-444.

11. Toll S, Manson JAE. An analysis of the compressibility of fiber assemblies. *In: Proceeding of the sixth International Conference on Fiber-Reinforced Composites, Institute of Materials*, Newcastle upon Tyne, UK, 1994, p. 25/1–25/10.

12. Mehri D, Michaud V, Comte E, Manson JAE. Predicting the sizing dependent rigidity of glass fibre bundles in sheet moulding compounds. *Composites Part A* 37 (2006) 1773-1786.

13. Luo Y, Verpoest I. Compressibility and relaxation of a new sandwich textile preform for liquid composite molding. *Polymer Composites* 20 (1999) 179-191.

14. Kelly PA, Umer R, Bickerton S. Viscoelastic response of dry and wet fibrous materials during infusion processes. *Composites Part A* 37 (2006) 868–873.

15. Press W.H., Teukolsky S.A., Vetterling W.T. and Flannery B.P., *Numerical recipes. 2nd edition*, Cambridge university press, 1992.

16. Drapier S, Pagot A, Vautrin A, Henrat P. Influence of the stitching density on the transverse permeability of non-crimped new concept (NC2) multiaxial reinforcements: measurements and predictions. *Composites Science and Technology* 62 (2002) 1979-1991.

17. Scholz S, Gillespie JW, Heider D. Measurement of transverse permeability using gaseous and liquid flow. *Composites Part A* 38 (2007): 2034-2040.

18. Ouagne P. and Bréard J. Continuous transverse permeability of fibrous media. Composites: Part A (2009), doi:10.1016/j.compositesa.2009.07.008.

Captions to Tables

Table 1: Governing equations for Hydro-Mechanical couplings analysis

Table 2: Compressibility parameters computed by inverse method

Equations		Dependent variables
Mass conservation (1)	$\frac{\partial q}{\partial z} = \frac{1}{V_f}\left(\frac{\partial V_f}{\partial t} + u_s \frac{\partial V_f}{\partial z}\right)$	q , V_f
Darcy's law (2)	$\nabla p = -\frac{\mu}{K_Z} q$	p , q , K_Z
Stress balance (3)	$\sigma'_Z - p = \sigma_Z$	σ'_Z , p
Stress-V_f Relationship (4)	$\sigma'_Z = F_c(V_f)$ With $F_c = cV_f^d$ (Toll and Manson's Equation)	V_f , σ'_Z
Permeability-V_f relationship (5)	$K_Z = F_p(V_f)$	V_f , K_Z
Total :	5 equations	5 variables

Table 1. Governing equations for Hydro-Mechanical couplings analysis

	Parameter *c*	Parameter *d*
Load (5 kN/min)	873	17,49
Load (10kN/min)	224	14,45

Table 2: Compressibility parameters computed by inverse method

Captions to Figures

Figure 1: Schematic diagram presenting the LCM processes (Bréard *et al.* [1])

Figure 2: Schematic of the Resin Film Infusion process (RFI)

Figure 3: The Hydro-Mechanical testing device

Figure 4: Linearity of the pressure-flow rate relationship

Figure 5: Transverse permeability of the 5 harness glass satin weave

Figure 6: Experimental Hydro-Mechanical coupling under stress conditions

Figure 7: Experimental Hydro-Mechanical loading and saturated compression under displacement condition

Figure 8: Influence of the compaction velocity on experimental and calculated using Ouahbi *et al.* model [2] compressibility curves

Figure 9: Validation of the Hydro-Mechanical model used with inverse method

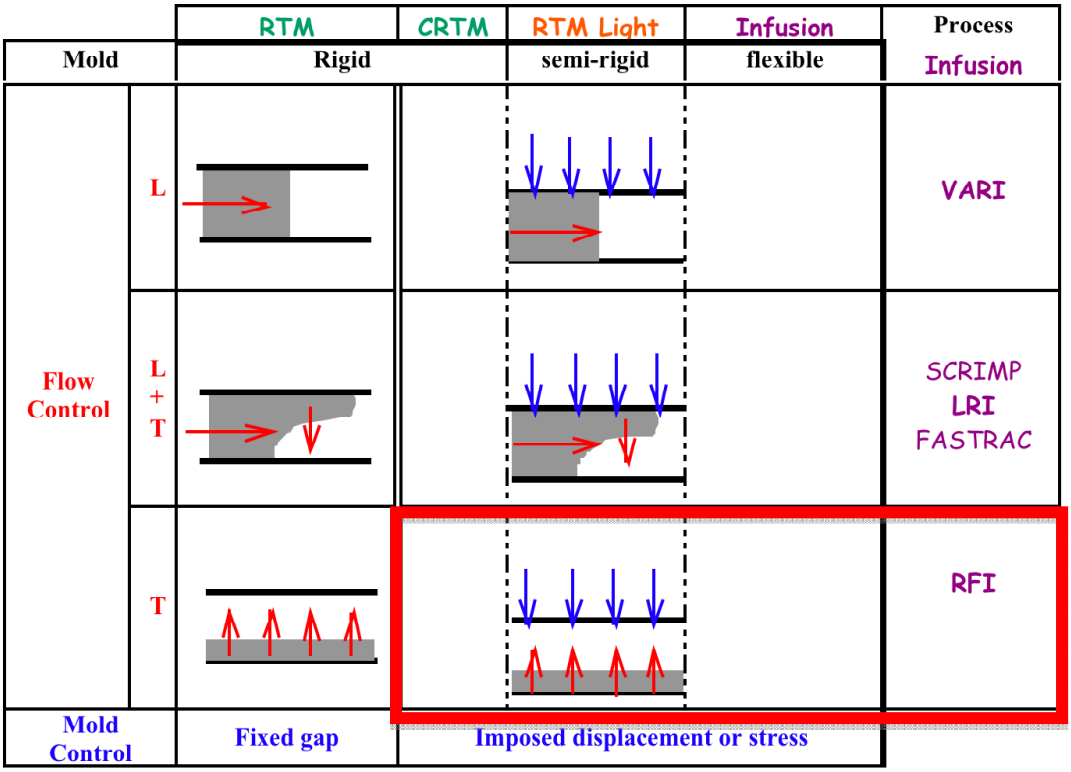

Figure 1: Schematic diagram presenting the LCM processes (Bréard *et al.* [1])

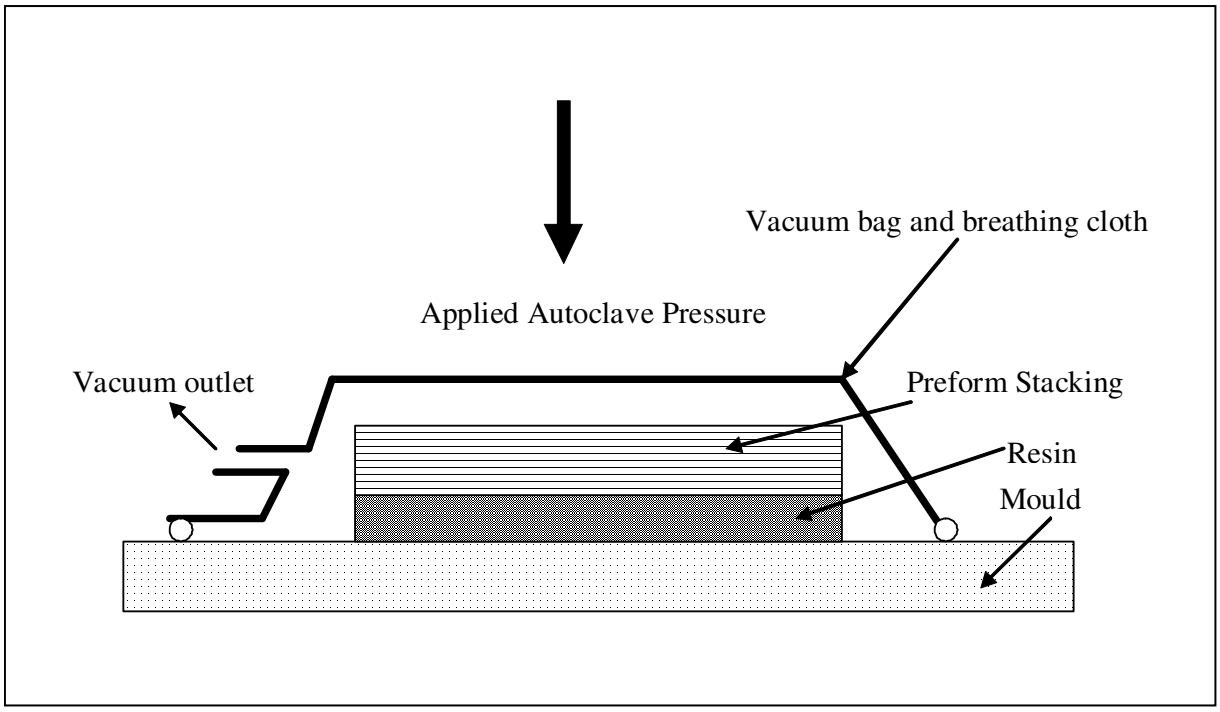

Figure 2: Schematic of the Resin Film Infusion process (RFI)

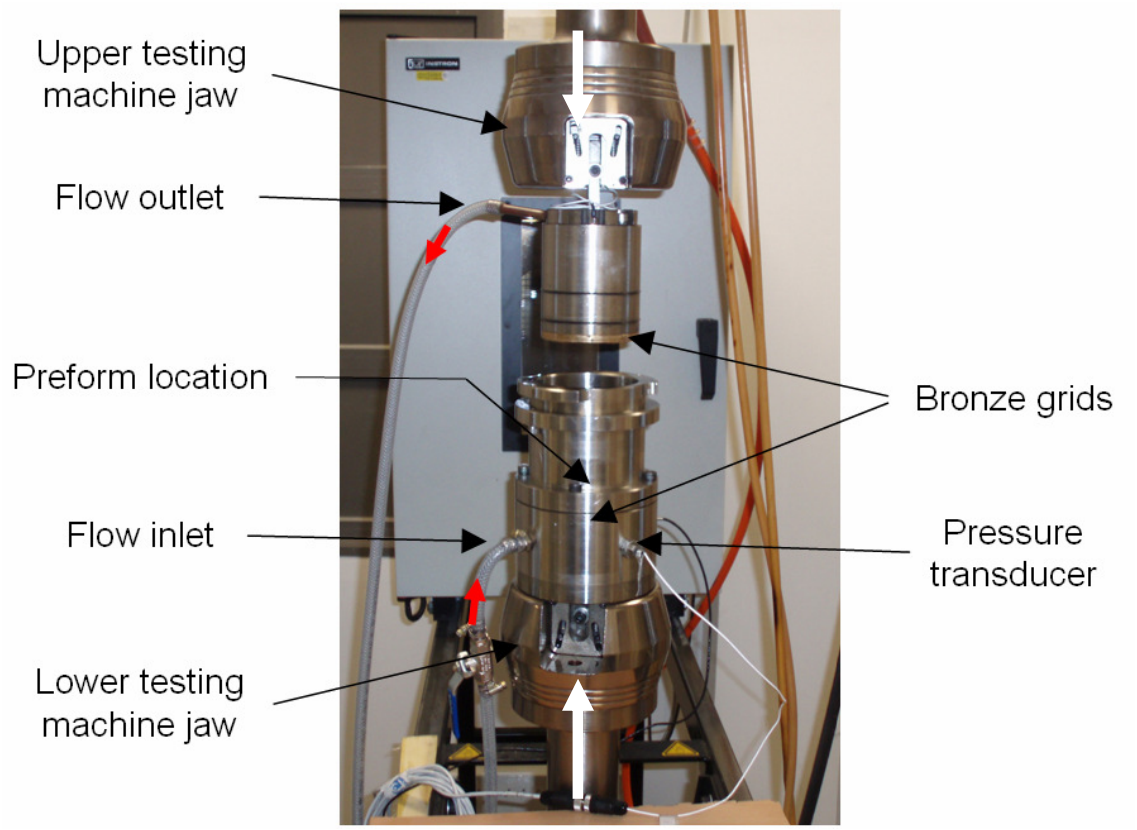

Figure 3: The Hydro-Mechanical testing device

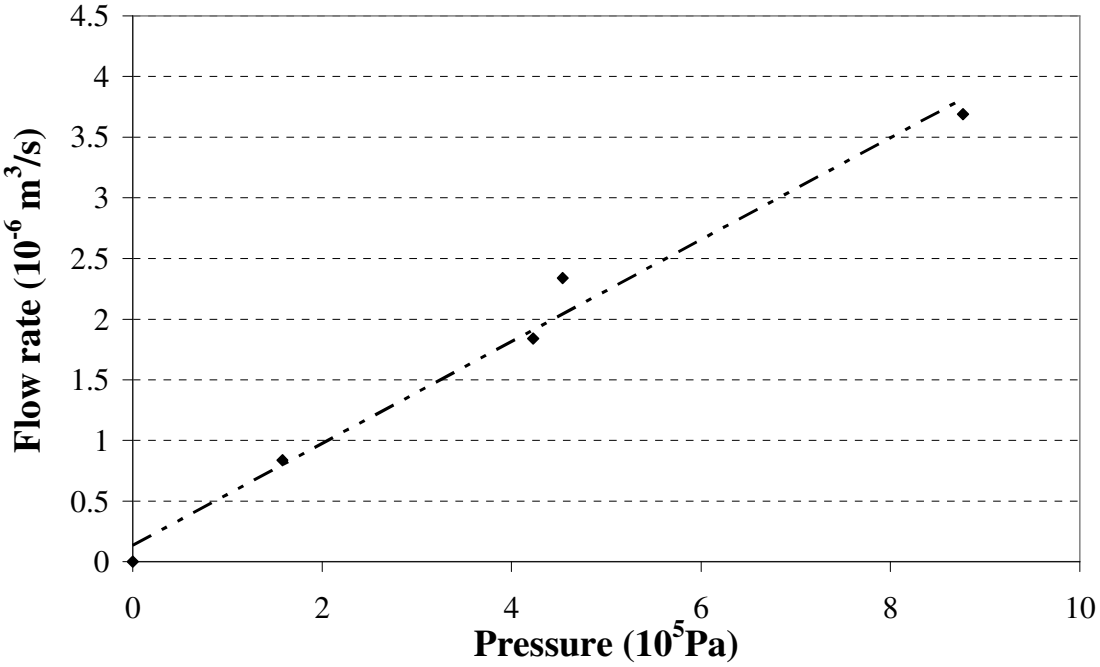

Figure 4: Linearity of the flow rate-pressure relationship

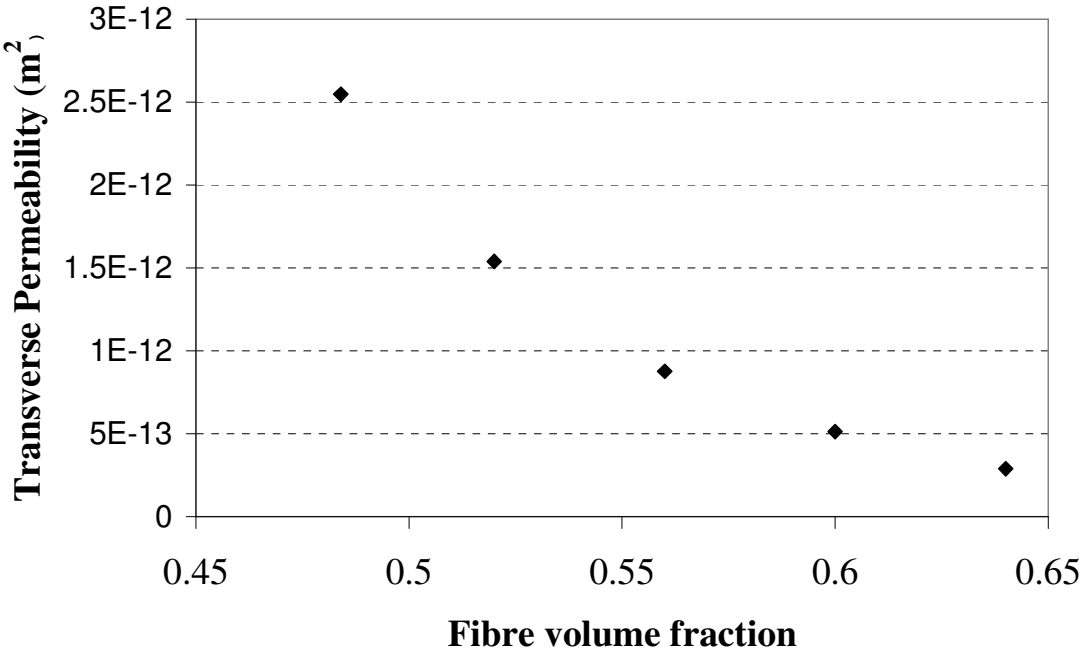

Figure 5: Transverse permeability of the 5 harness glass satin weave

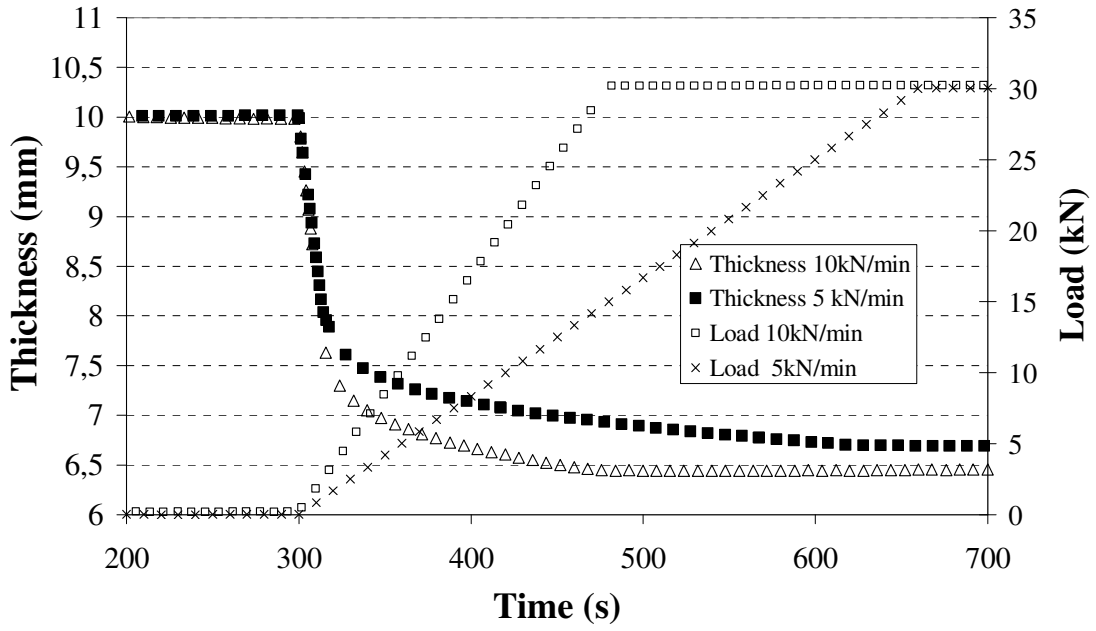

Figure 6: Experimental Hydro-Mechanical coupling under stress conditions

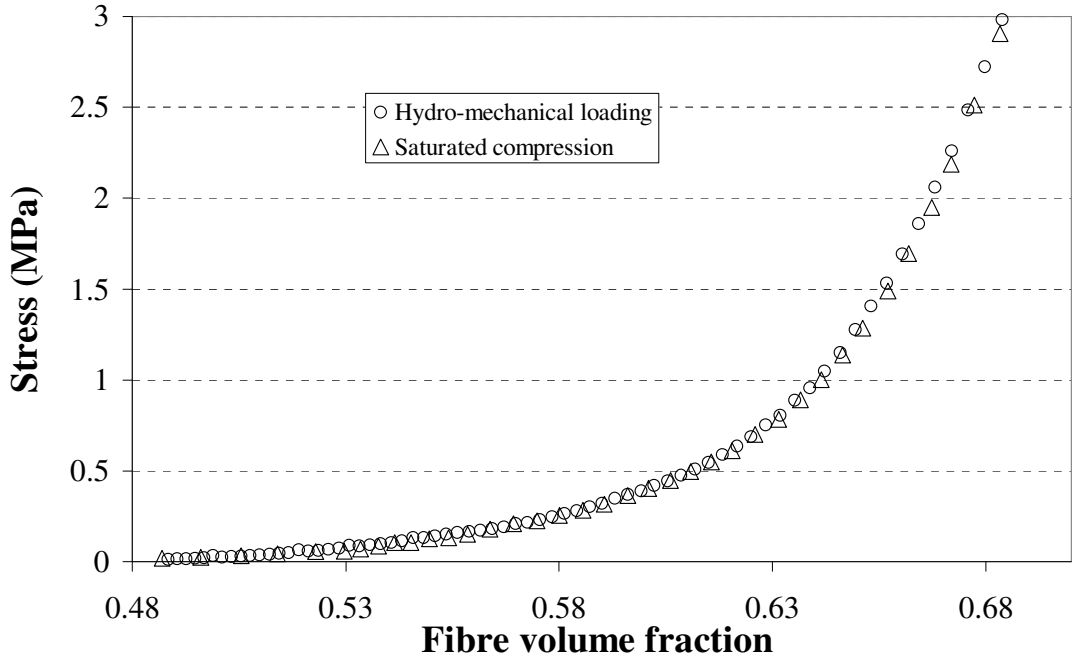

Figure 7: Experimental Hydro-Mechanical loading and saturated compression under displacement condition

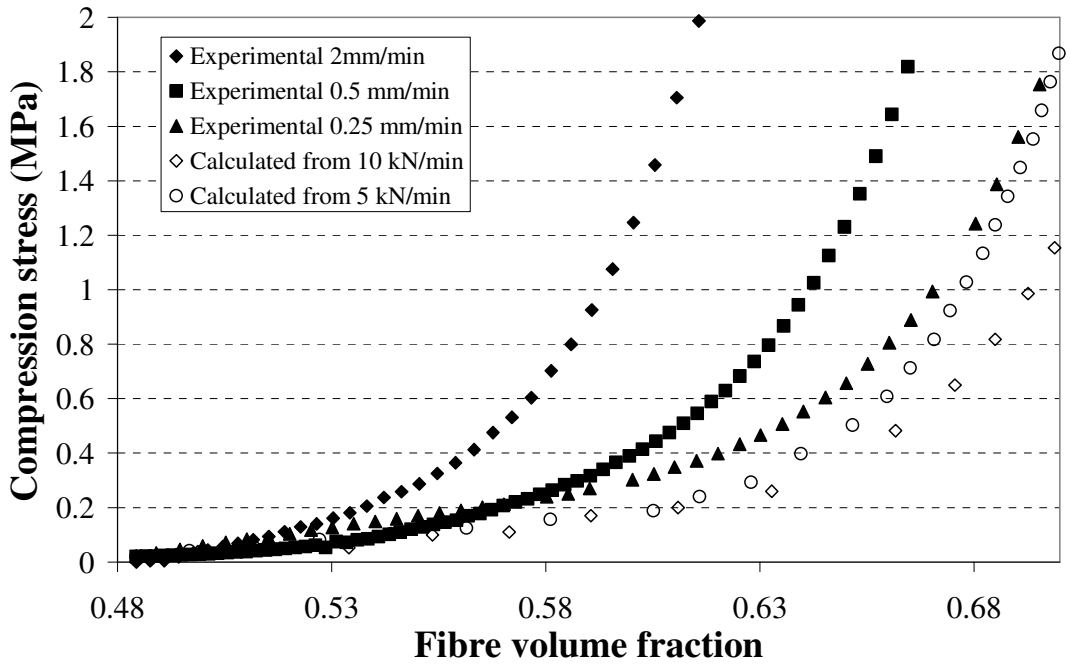

Figure 8: Influence of the compaction velocity on experimental and calculated using Ouahbi *et al.* model [2] compressibility curves

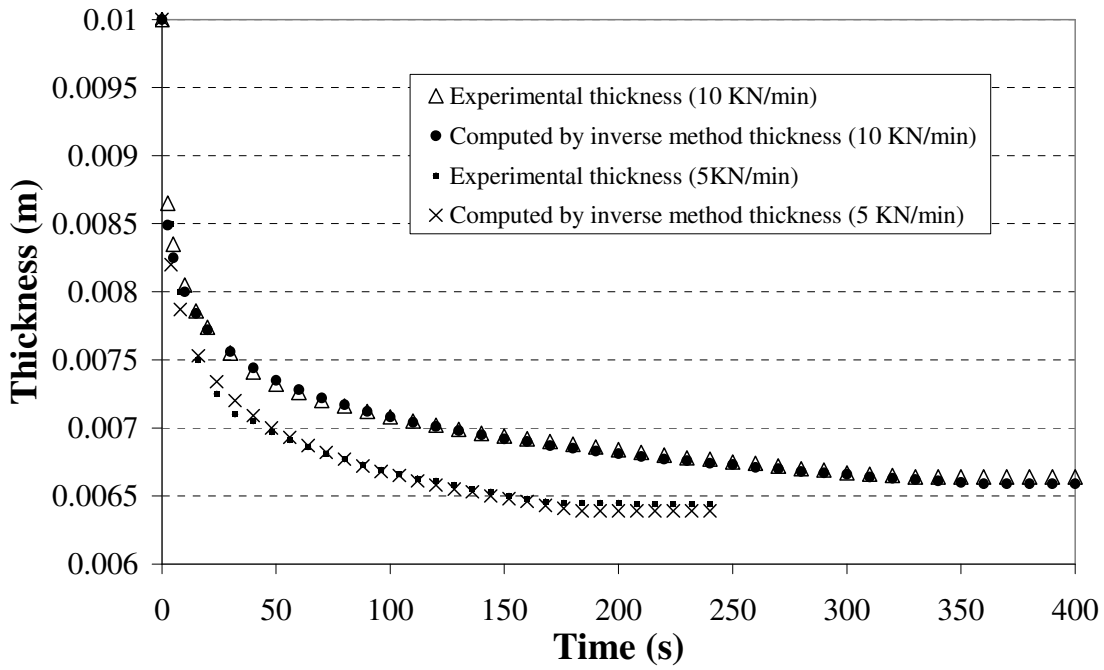

Figure 9: Validation of the Hydro-Mechanical model used with inverse method

Appendix A : The mass conservation equations of resin and fibre, in transverse analysis, can be written respectively as:

Fluid phase
$$\frac{\partial \phi}{\partial t} + \frac{\partial}{\partial z}\left(\phi \frac{\partial V}{\partial t} \right) = 0 \tag{A.1}$$

Solid phase
$$\frac{\partial (1-\phi)}{\partial t} + \frac{\partial}{\partial z}\left((1-\phi) \frac{\partial U}{\partial t} \right) = 0 \tag{A.2}$$

Where ϕ is the porosity of the medium, with $\phi = 1 - V_f$, V the displacement of the fluid and U the displacement of the reinforcement.

The relative displacement of fluid W is defined by: $W(M,t) = V(M,t) - U(M,t)$

Equation (A.1) can be rewritten using the relative displacement of fluid:

$$\frac{\partial \phi}{\partial t} + \frac{\partial}{\partial z}\left(\phi \frac{\partial W}{\partial t} + \phi \frac{\partial U}{\partial t} \right) = 0 \tag{A.3}$$

The velocities are introduced: $u_s = \frac{\partial U}{\partial t}$, $q_f = \frac{\partial V}{\partial t}$ and $q = \phi \frac{\partial W}{\partial t}$

Equation (A.3) can be expressed as a function of the velocities:

$$\frac{\partial \phi}{\partial t} + \frac{\partial q}{\partial z} + \phi \frac{\partial u_s}{\partial z} + u_s \frac{\partial \phi}{\partial z} = 0 \tag{A.4}$$

Solid phase equation (A.2) can be expressed as:

$$\frac{\partial (1-\phi)}{\partial t} + (1-\phi) \frac{\partial u_s}{\partial z} - u_s \frac{\partial \phi}{\partial z} = 0 \tag{A.5}$$

The mass conservation equation is described by the following combination of equations (A.4) and (A.5): $(1-\phi) \cdot (A.4) - (\phi) \cdot (A.5)$

$$\frac{\partial q}{\partial z} = -\frac{1}{1-\phi}\left(\frac{\partial \phi}{\partial t} + u_s \frac{\partial \phi}{\partial z} \right) \tag{A.6}$$

Equation (A.6) can be expressed as a function of fibre volume fraction as $\frac{\partial V_f}{\partial t} = -\frac{\partial \phi}{\partial t}$:

$$\frac{\partial q}{\partial z} = \frac{1}{V_f}\left(\frac{\partial V_f}{\partial t} + u_s \frac{\partial V_f}{\partial z} \right) \tag{A.7}$$

It can be shown that $\frac{1}{V_f}\frac{\partial V_f}{\partial z}u_s$ can be neglected in comparison to the other term of the governing equation $\frac{1}{V_f}\frac{\partial V_f}{\partial t}$. To demonstrate this, a non dimensional number $\beta = \left(\frac{\partial V_f}{\partial z}u_s\right) / \left(\frac{\partial V_f}{\partial t}\right)$ is plotted as a function of the compression speed and the evolution of the thickness (from 1 no compression to 0 that corresponds to a full compression ie: no space for the reinforcement).

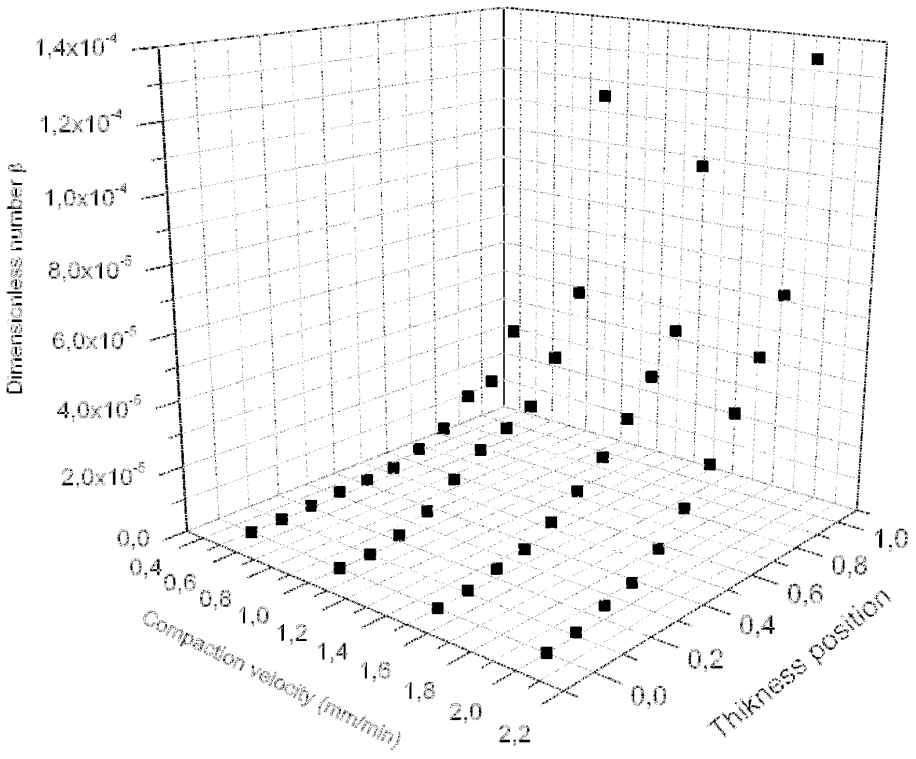

In any of the plotted conditions, the value of β is very low (in the 10^{-4}) range, and therefore it is normal to neglect the term $\frac{1}{V_f}\frac{\partial V_f}{\partial z}u_s$ in comparison to the term $\frac{1}{V_f}\frac{\partial V_f}{\partial t}$ in the sum of the governing equation.

Equation (A.7) can therefore be simplified:

$$\frac{\partial q}{\partial z} = \frac{1}{V_f}\left(\frac{\partial V_f}{\partial t}\right) \tag{A.8}$$